NIOBOKUPLETSKITE, A NEW ASTROPHYLLITE-GROUP MINERAL
FROM MONT SAINT-HILAIRE, QUEBEC, CANADA:
DESCRIPTION AND CRYSTAL STRUCTURE

PAULA C. PIILONEN[§] AND ANDRÉ E. LALONDE

Ottawa–Carleton Geoscience Centre, Department of Earth Sciences, University of Ottawa, Ottawa, Ontario K1N 6N5, Canada

ANDREW M. McDONALD

Department of Earth Sciences, Laurentian University, Sudbury, Ontario P3E 2C6, Canada

ROBERT A. GAULT

Research Division, Canadian Museum of Nature, P.O. Box 3443, Station D, Ottawa, Ontario K1P 6P4, Canada

ABSTRACT

Niobokupletskite is a new member of the astrophyllite group found in nepheline syenite pegmatites at Mont Saint-Hilaire, Quebec, in association with aegirine, albite, analcime, calcio-ancylite-(Ce), calcite, catapleiite, epididymite, fluorite, genthelvite, microcline, natrolite, pyrochlore, rhodochrosite and wurtzite. It is transparent, with a vitreous luster, brittle with a perfect {001} cleavage, and has an uneven to splintery fracture. Niobokupletskite is biaxial positive, α 1.718(1), β 1.733(1), γ_{calc} 1.750(1), $2V_{meas} = 87(2)°$. It is triclinic, $P\bar{1}$, a 5.4303(9), b 11.924(2), c 11.747(2) Å, α 112.927(3), β 94.750(3), γ 103.175(3)°, V 669.5(3) Å^3. The average result of three electron-microprobe analyses is: Na$_2$O 2.62, K$_2$O 5.97, Rb$_2$O 0.82, Cs$_2$O 0.12, MgO 0.15, MnO 26.37, FeO 2.64, ZnO 4.08, Al$_2$O$_3$ 1.14, TiO$_2$ 1.34, ZrO$_2$ 3.43, Nb$_2$O$_5$ 12.13, Ta$_2$O$_5$ 0.63, SiO$_2$ 31.85, F 0.14, H$_2$O(calc.) 2.48, total 95.85 wt.%, corresponding to (K$_{1.84}$Rb$_{0.13}$Cs$_{0.01}$)$_{\Sigma 1.98}$Na$_{0.95}$ (Mn$_{5.40}$Zn$_{0.73}$Fe$_{0.53}$Na$_{0.28}$Mg$_{0.05}$)$_{\Sigma 6.99}$ (Nb$_{1.33}$Zr$_{0.40}$Ti$_{0.24}$Ta$_{0.04}$)$_{\Sigma 2.01}$ (Si$_{7.71}$Al$_{0.32}$)$_{\Sigma 8.03}$ O$_{26}$(OH)$_{4.00}$(O$_{0.89}$F$_{0.11}$)$_{\Sigma 1.00}$ on the basis of 31 anions, or, ideally, K$_2$Na(Mn,Zn,Fe)$_7$(Nb,Zr,Ti)$_2$Si$_8$O$_{26}$(OH)$_4$(O,F). Niobokupletskite is a heterophyllosilicate with a *HOH*-structure consisting of a sheet of close-packed octahedra (*O*-sheet) sandwiched between two heterogeneous sheets (*H*-sheets) with a Si:Nb ratio of 4:1. It forms a solid-solution series with kupletskite *via* the coupled substitution Ti^{4+} + F$^-$ or OH$^-$ ⇔ Nb^{5+} + O^{2-}. Niobokupletskite is a postmagmatic phase and possibly the result of late-stage remobilization of Nb *via* late oxidized aqueous fluids.

Keywords: niobokupletskite, astrophyllite-group mineral, new mineral species, crystal structure, heterophyllosilicate, solid-solution series, kupletskite, Mont Saint-Hilaire, Quebec.

SOMMAIRE

La niobokupletskite est une nouvelle espèce minérale, membre du groupe de l'astrophyllite, que l'on retrouve dans les pegmatites syénitiques à néphéline du Mont Saint-Hilaire, Québec, en association avec aegyrine, analcime, calcite, catapléite, épididymite, fluorite, genthelvite, microcline, natrolite, pyrochlore, rhodochrosite et wurtzite. C'est un minéral transparent, avec éclat vitreux, cassant, avec un clivage {001} parfait et une fracture irrégulière à fibreuse. La niobokupletskite est biaxe positive, avec α 1.718(1), β 1.733(1), γ_{calc} 1.750(1), $2V_{observé} = 87(2)°$. Le minéral est triclinique, groupe spatial $P\bar{1}$, avec paramètres réticulaires a 5.4303(9), b 11.924(2), c 11.747(2) Å, α 112. 927(3), β 94.750(3), γ 103.175(3)°, et V 669.5(3) Å^3. La moyenne de trois déterminations de la composition par microsonde électronique a donné: Na$_2$O 2.62, K$_2$O 5.97, Rb$_2$O 0.82, Cs$_2$O 0.12, MgO 0.15, MnO 26.37, FeO 2.64, ZnO 4.08, Al$_2$O$_3$ 1.14, TiO$_2$ 1.34, ZrO$_2$ 3.43, Nb$_2$O$_5$ 12.13, Ta$_2$O$_5$ 0.63, SiO$_2$ 31.85, F 0.14, H$_2$O(calc.) 2.48, somme 95.85% en poids, ce qui correspond à la formule structurale (K$_{1.84}$Rb$_{0.13}$Cs$_{0.01}$)$_{\Sigma 1.98}$Na$_{0.95}$(Mn$_{5.40}$Zn$_{0.73}$Fe$_{0.53}$Na$_{0.28}$Mg$_{0.05}$)$_{\Sigma 6.99}$ (Nb$_{1.33}$Zr$_{0.40}$Ti$_{0.24}$Ta$_{0.04}$)$_{\Sigma 2.01}$ (Si$_{7.71}$Al$_{0.32}$)$_{\Sigma 8.03}$O$_{26}$(OH)$_{4.00}$(O$_{0.89}$F$_{0.11}$)$_{\Sigma 1.00}$ sur une base de 31 anions, ou, de façon idéale, K$_2$Na(Mn,Zn,Fe)$_7$(Nb,Zr,Ti)$_2$Si$_8$O$_{26}$(OH)$_4$(O,F). La niobokupletskite est un hétérophyllosilicate ayant une struture *HOH* composée d'une couche d'octaèdres avec entassement maximal se retrouvant entre deux couches hétérogènes (couches *H*) ayant un rapport Si:Nb de 4:1. Elle fait partie d'une solution solide avec la kupletskite selon la substitution Ti^{4+} + F$^-$ ou OH$^-$ ⇔ Nb^{5+} + O^{2-}. La niobokupletskite est d'origine postmagmatique et provient possiblement d'une remobilisation tardive du Nb par le biais d'une phase aqueuse tardive oxydée.

Mots-clés: niobokupletskite, minéral du groupe de l'astrophyllite, Mont Saint-Hilaire, Québec, nouvelle espèce minérale, structure cristalline, hétérophyllosilicate, solution solide, kupletskite.

§ *E-mail address*: ppiilon@science.uottawa.ca

INTRODUCTION

Niobokupletskite, ideally $K_2Na(Mn,Zn,Fe)_7$ $(Nb,Zr,Ti)_2Si_8O_{26}(OH)_4(O,F)$, is a new member of the astrophyllite group discovered in the nepheline syenite pegmatites in the Poudrette Quarry at Mont Saint-Hilaire, Québec. With the addition of niobokupletskite, the Nb-dominant analogue of kupletskite, eight species of astrophyllite-group minerals are now recognized (Table 1). Niobokupletskite is the third member of the astrophyllite group, along with astrophyllite and kupletskite, to be described from this locality (Horváth & Gault 1990). The name niobokupletskite comes from the fact that it is the Nb-analogue of kupletskite (Semenov 1956). The mineral species and the name have been approved by the IMA Commission on New Minerals and New Mineral Names. Holotype material has been deposited at the Canadian Museum of Nature, Ottawa (catalogue no. CMNMC 82924). The purpose in this paper is to describe niobokupletskite, discuss its structure in relation to kupletskite, and to comment on its paragenesis. Extensive information concerning the structure and chemical variations of a large suite of astrophyllite-group minerals, including niobokupletskite, will be presented in future papers.

OCCURRENCE AND DESCRIPTION

Mont Saint-Hilaire (MSH), located 40 km east of Montreal, Quebec, is one of ten early Cretaceous alkaline intrusions collectively referred to as the Monteregian Hills (Adams 1903). The peralkaline East Hill Suite is host to a variety of petrological microenvironments (Piilonen et al. 1998), all of which contain astrophyllite-group minerals except for the so-called marble xenoliths. Niobokupletskite occurs in nepheline syenite pegmatites as a late-stage mineral.

Three distinct types of niobokupletskite have been discovered, each with its own specific occurrence and associated mineral assemblage. Type-I niobokupletskite (holotype material) occurs as anhedral to subhedral, platy to tabular, light beige to yellow epitaxic overgrowths on primary, dark brown kupletskite associated with aegirine, albite, microcline and pyrochlore. The primary kupletskite is zoned; it possesses a relatively Ti-rich core and a Nb-enriched rim; this zonation is indicated by an arrow in Figure 1B, with dark zones in this back-scattered electron (BSE) image corresponding to Ti-enrichment, and light zones indication of Nb-enrichment. Type-II niobokupletskite occurs as a dense, fibrous, light yellow-brown overgrowth on coarse-
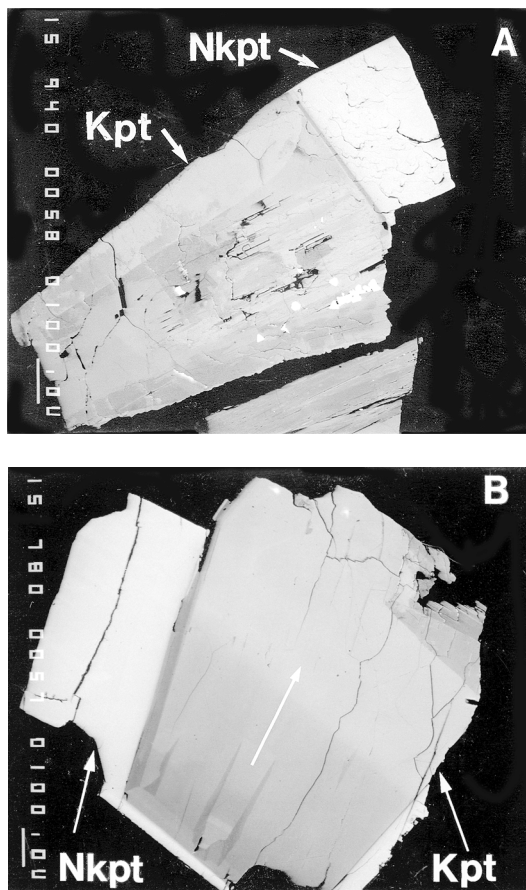
FIG. 1. Back-scattered electron images of type-I niobokupletskite. A. Nb-rich kupletskite (Kpt, dark grey) with irregular zonation and a sharp contact with niobokupletskite (Nkpt, light grey). Note the pyrochlore inclusions (white) along fractures in the kupletskite. B. Niobokupletskite (Nkpt) rimming kupletskite (Kpt). The zoning in the kupletskite is from Nb-poor to Nb-rich in the direction of the arrow (dark to medium grey). Scale bar: 100 μm.

TABLE 1. MEMBERS OF THE ASTROPHYLLITE GROUP

Species	Formula
[1] Niobokupletskite	$K_2Na(Mn,Zn,Fe)_7(Nb,Zr,Ti)_2Si_8O_{26}(OH)_4(O,F)$
[2] Kupletskite	$(K,Na)_3(Mn,Fe^{2+})_7(Ti,Nb)_2Si_8O_{24}(O,OH)_7$
[3] Cesium-kupletskite	$(Cs,K,Na)_3(Mn,Fe,Li)_7(Ti,Nb)_2Si_8O_{24}(O,OH,F)_7$
[4] Astrophyllite	$(K,Na)_3(Fe^{2+},Mn)_7Ti_2Si_8O_{24}(O,OH)_7$
[5] Magnesium astrophyllite	$K_2NaNa(Fe,Mn)_4Mg_2Ti_2Si_8O_{24}(OH)_4(OH,F)_2$
[6] Niobophyllite	$(K,Na)_3(Fe^{2+},Mn)_6(Nb,Ti)_2Si_8O_{26}(O,OH,F)_7$
[7] Zircophyllite	$(K,Na,Ca)_3(Mn,Fe^{2+})_7(Zr,Nb)_2Si_8O_{27}(OH,F)_4$
[8] Hydroastrophyllite	$(H_3O,K,Ca)_3(Fe^{2+},Mn)_{5-6}Si_8Si_8(O,OH)_{31}$

[1] this study, [2] Semenov (1956), [3] Efimov et al. (1971), [4] Peng & Ma (1963), [5] Shi et al. (1998), [6] Nickel et al. (1965), [7] Kapustin 1973, [8] Hubei Geological College (1974).

grained primary kupletskite associated with primary and secondary aegirine, albite, calcio-ancylite-(Ce), catapleiite, microcline, natrolite, pyrochlore and rhodochrosite. Type-III niobokupletskite occurs as an overgrowth on primary kupletskite as very fine-grained bronze to silvery brown acicular crystals in sheaf-like aggregates, originally described as "witch's broom astrophyllite" (Wight & Chao 1986). Type-III niobokupletskite is associated with primary and secondary aegirine, albite, analcime, calcio-ancylite-(Ce), calcite, catapleiite, epididymite, fluorite, genthelvite, microcline, natrolite, pyrochlore, rhodochrosite, and wurtzite.

Niobokupletskite has a perfect {001} cleavage, is vitreous, brittle, and has an uneven to splintery fracture. It does not fluoresce under either short- or long-wave ultraviolet light. It has a Mohs hardness of 3 to 4. Niobokupletskite sinks in methylene iodide (density of 3.325 g/cm^3) and has a calculated density of 3.46 g/cm^3.

Niobokupletskite is biaxial positive, with indices of refraction α 1.718(1), β 1.733(1), and γ_{calc} 1.750 (for λ = 598 nm); $2V_{meas}$ = 87(2)° (Kamb's method). A measured value for γ could not be obtained owing to the orientation of the selected grain on the spindle. The optical orientation is $Z = c$ with X and Y in the (001) plane. It is pleochroic with $X \approx Y$ light orange-yellow, and Z red-brown. A Gladstone–Dale calculation gives a compatibility index of 0.005, which is regarded as superior (Mandarino 1981).

CHEMICAL COMPOSITION

Chemical analyses of type-I, -II and -III niobokupletskite were done on a JEOL 733 electron microprobe at the Canadian Museum of Nature using Tracor Northern 5500 and 5600 automation in wavelength-dispersion mode. The operating conditions were as follows: beam diameter 20 μm, operating voltage 15 kV, and a beam current of 20 nA. Data reduction was performed using a PAP routine in XMAQNT (C. Davidson, CSIRO). Overlap corrections for Si($K\alpha$)–Sr($L\alpha$), Zr($L\beta$)–Nb($L\alpha$) and Mn($K\beta$)–Nb($L\alpha$) were done. A total of 24 elements were sought, and the following standards were employed: Na-amphibole (Na$K\alpha$, Si$K\alpha$), sanidine (K$K\alpha$, Al$K\alpha$), diopside (Ca$K\alpha$, Mg$K\alpha$), tephroite (Mn$K\alpha$), almandine (Fe$K\alpha$), rutile (Ti$K\alpha$), synthetic MnNb$_2$O$_6$ (Nb$L\alpha$), vlasovite (Zr$L\alpha$), zincite (Zn$L\alpha$), phlogopite (F$K\alpha$), pollucite (Cs$L\alpha$), celestite (Sr$L\alpha$), sanbornite (Ba$L\alpha$), synthetic rubicline (Rb$L\alpha$), synthetic NiTa$_2$O$_6$ (Ta$M\alpha$), and hafnon (Hf$M\alpha$). Count times for all elements were 25 seconds or 0.5% precision, whichever was obtained first, except for Cs and Rb (100 seconds), and Hf (50 seconds). Also sought but not detected were La, Ce, Yb, P, Th, Pb, Ni, V, U, W, Sc, S and Mo. Complete electron-microprobe data can be found in Table 2. Chemical formulae were calculated on the basis of 31 anions, as determined during crystal-structure analysis. The average of three compositions of type-I niobokupletskite gives the empirical formula (K$_{1.84}$
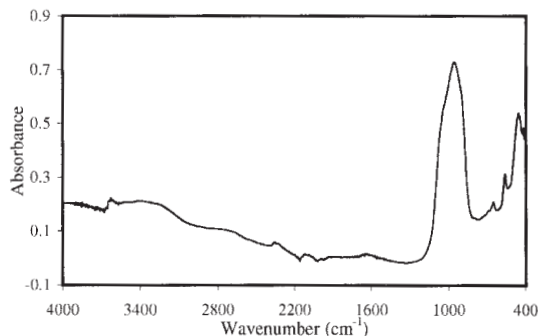

FIG. 2. Infrared transmittance spectrum of niobokupletskite.

Rb$_{0.13}$Cs$_{0.01}$)$_{\Sigma 1.98}$ Na$_{0.95}$(Mn$_{5.40}$Zn$_{0.73}$Fe$_{0.53}$Na$_{0.28}$ Mg$_{0.05}$)$_{\Sigma 6.99}$ (Nb$_{1.33}$Zr$_{0.40}$Ti$_{0.24}$Ta$_{0.04}$)$_{\Sigma 2.01}$ (Si$_{7.71}$Al$_{0.32}$) $_{\Sigma 8.03}$ O$_{26}$(OH)$_{4.00}$(O$_{0.89}$F$_{0.11}$)$_{\Sigma 1.00}$, or, ideally, K$_2$Na (Mn,Zn,Fe)$_7$ (Nb,Zr,Ti)$_2$Si$_8$O$_{26}$ (OH)$_4$(O,F). Chemically, type-II and type-III niobokupletskite differ from the type material only by being deficient in Zn (<0.04 atoms per formula unit, *apfu*, Table 2).

INFRARED ANALYSIS

The infrared spectrum of niobokupletskite was obtained using a Bomem Michelson MB–100 Fourier transform infrared spectrometer equipped with a mercury cadmium telluride (MCT) detector. A single crystal of the type material was initially dried in an oven at 50°C for 30 minutes, mounted in a diamond-anvil microsample cell, and the spectrum collected over the range of 4000 to 400 cm^{-1}. The absorbance spectrum (Fig. 2) shows broad peaks in the high-frequency range (4000 to 1000 cm^{-1}) attributable to O–H stretching (3626 cm^{-1} and associated shoulder centered at 3396 cm^{-1}), and a weak peak at 1647 cm^{-1} attributable to H–O–H bending of absorbed or molecular H$_2$O (Farmer 1974). The lack of recognizable H$_2$O in the structure refinement suggests that this contribution is likely due to adsorbed water not driven off during the drying process. The middle- to lower-frequency end of the spectrum (1000 to 400 cm^{-1}) is characterized by symmetric Si–O stretching (964 and 812 cm^{-1}) and bending (696 and 654 cm^{-1}). Low-frequency bands at 457, 418 and 405 cm^{-1} can be attributed to Mn–O stretching (Farmer 1974).

MÖSSBAUER SPECTROSCOPY

The wide range of chemical compositions and the presence of structural vacancies preclude the possibility of using stoichiometry to calculate Fe^{2+}/Fe^{3+} values in astrophyllite-group minerals. Mössbauer spectroscopy was therefore employed to determine the proportion and distribution of Fe^{2+} and Fe^{3+} in niobokupletskite

TABLE 2. CHEMICAL COMPOSITION OF NIOBOKUPLETSKITE*, MONT SAINT-HILAIRE, QUEBEC

Oxide	TYPE I				TYPE II	TYPE III	Oxide	TYPE I				TYPE II	TYPE III
	1	2	3	Ave.				1	2	3	Ave.		
Na₂O wt.%	2.69	2.49	2.67	2.62	2.37	2.66		Formula based on 31 anions					
K₂O	6.03	5.92	5.95	5.97	6.04	5.76	K apfu	1.85	1.83	1.84	1.84	1.83	1.75
Rb₂O	0.82	0.81	0.84	0.82	0.66	0.91	Rb	0.13	0.13	0.13	0.13	0.10	0.14
Cs₂O	0.12	0.13	0.10	0.12	0.00	0.00	Cs	0.01	0.01	0.01	0.01	0.00	0.00
CaO	0.00	0.00	0.00	0.00	0.10	0.03	Sr	0.00	0.00	0.00	0.00	0.01	0.00
SrO	0.00	0.00	0.00	0.00	0.04	0.00	Na	0.00	0.00	0.00	0.00	0.07	0.19
MgO	0.13	0.15	0.18	0.15	0.18	0.43	Sum A	1.99	1.97	1.99	1.98	2.01	2.08
MnO	26.11	26.40	26.61	26.37	26.60	30.13							
FeO	2.63	2.73	2.55	2.64	7.44	3.71							
ZnO	4.31	4.29	3.65	4.08	0.25	0.00	Na	0.90	0.98	0.97	0.95	1.04	1.18
Al₂O₃	1.21	1.02	1.20	1.14	1.18	1.69	Ca	0.00	0.00	0.00	0.00	0.03	0.01
TiO₂	1.12	1.26	1.65	1.34	1.63	1.67	Sum B	0.90	0.98	0.97	0.95	1.00	1.00
ZrO₂	3.23	4.23	2.84	3.43	4.80	3.56							
HfO₂	0.00	0.00	0.00	0.00	0.04	0.00	Na	0.35	0.20	0.29	0.28	0.05	0.05
Nb₂O₅	12.84	11.54	12.00	12.13	10.64	11.40	Mg	0.05	0.05	0.07	0.05	0.06	0.15
Ta₂O₅	0.44	0.74	0.71	0.63	0.48	0.25	Mn	5.31	5.43	5.48	5.40	5.36	6.06
SiO₂	31.93	31.80	31.82	31.85	32.06	31.86	Fe²⁺	0.53	0.55	0.52	0.53	1.48	0.74
F	0.43	0.00	0.00	0.14	0.34	0.29	Zn	0.76	0.77	0.66	0.73	0.04	0.00
H₂O	2.50	2.47	2.47	2.48	2.52	2.52	Sum C	7.00	7.00	7.00	7.00	7.00	7.00
O=F	-0.18	0.00	0.00	-0.06	-0.14	-0.12	Ti	0.20	0.23	0.30	0.24	0.29	0.30
							Zr	0.38	0.50	0.34	0.41	0.56	0.41
Total	96.36	95.98	95.24	95.85	97.23	96.75	Hf	0.00	0.00	0.00	0.00	0.00	0.00
							Nb	1.39	1.27	1.32	1.33	1.14	1.23
							Ta	0.03	0.05	0.05	0.04	0.03	0.02
							Sum D	2.00	2.05	2.00	2.02	2.03	1.95
							Si	7.67	7.72	7.73	7.71	7.62	7.57
							Al	0.34	0.29	0.34	0.33	0.33	0.47
							Sum T	8.01	8.01	8.08	8.03	7.96	8.04
							O	26.67	27.00	27.00	26.89	26.74	26.78
							OH	4.00	4.00	4.00	4.00	4.00	4.00
							F	0.33	0.00	0.00	0.11	0.26	0.22
							Σ anions	31.00	31.00	31.00	31.00	31.00	31.00
							Σ cations	19.90	20.01	20.03	19.98	19.98	20.07

* Electron-microprobe data.

and to shed light on the oxidation conditions at the time of crystallization. Insufficient quantities of holotype (type-I) niobokupletskite precluded the possibility of obtaining a Mössbauer spectrum; an absorber for a sample of fibrous type-II niobokupletskite was therefore prepared by crushing an ideal mass of sample [55.1 mg, calculated using the technique of Rancourt *et al.* (1993)]. Crushing was done in acetone to minimize oxidation in the presence of atmospheric oxygen. The powdered niobokupletskite was suspended in petroleum jelly to ensure a random orientation of crystals within the circular aluminum mount (aperture: 1.0 cm, thickness: 0.6 cm).

The spectrum was obtained using a ^{57}Co source in a rhodium matrix at room temperature (21°C). The transducer was employed in constant-acceleration mode over a Doppler velocity range of ±4.0 mm/s, with fixed distances between the absorber and source and between the absorber and detector of 3.0 and 7.0 cm, respectively. Spectra were calibrated with an ^{57}Fe-enriched iron foil. Data were collected in 1024 channels and folded to obtain a flat background. Spectra were fitted with the Voigt-based quadrupole-splitting distribution method of Rancourt & Ping (1991), as implemented in the program RECOIL (Lagarec & Rancourt 1998).

The Mössbauer spectrum of niobokupletskite is shown in Figure 3, and the site-distribution parameters and associated errors, in Table 3. The spectrum is characterized by three main absorption peaks at approximately –0.07, 0.81 and 2.33 mm/s, corresponding to: (1) the sum of the low-energy lines from $^{[6]}Fe^{2+}$ and $^{[6]}Fe^{3+}$ doublets, (2) the high-energy lines from $^{[6]}Fe^{3+}$ doublets, and (3) the high-energy lines from $^{[6]}Fe^{2+}$ doublets, respectively. All Fe is found to be located in the sheet of octahedra (see below). The dominant feature in the spectrum is a wide doublet, attributable to $^{[6]}Fe^{2+}$ (modeled as having three Gaussian components), which has an average center shift (CS) of 1.13 mm/s (with respect to α-Fe at room temperature) and an average quadrupole-splitting distribution (QSD) of 2.33 mm/s. The low-energy side of this doublet displays a pronounced shoulder as a result of the presence
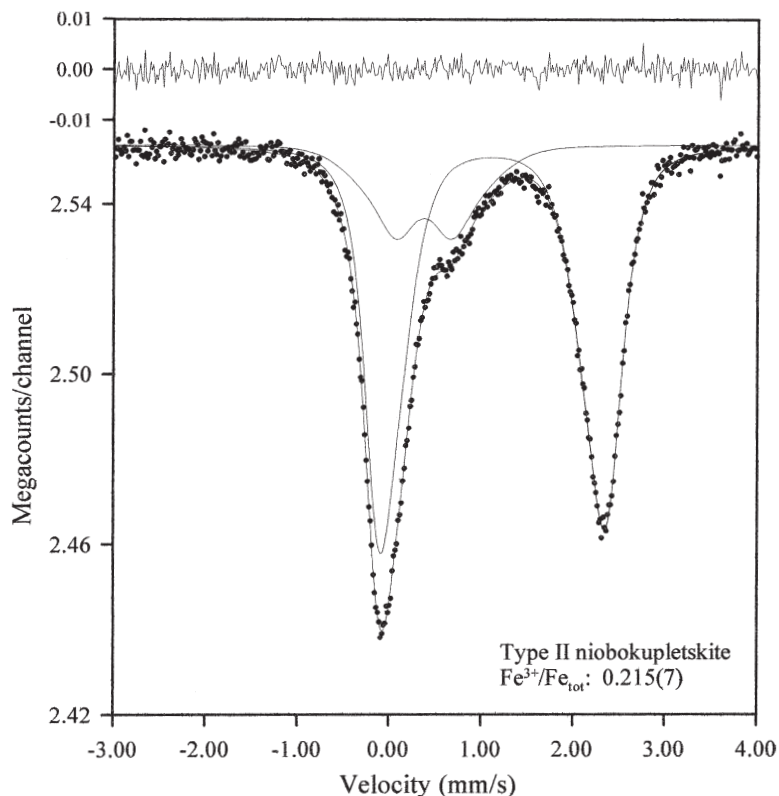
FIG. 3. Mössbauer spectrum of Type-II niobokupletskite. The solid line through the spectral data represents the best fit. The subspectral contributions corresponding to $^{[6]}Fe^{2+}$ and $^{[6]}Fe^{3+}$ are shown superimposed on the data. The difference between the observed and calculated spectrum is shown on an exaggerated vertical scale at the top of the figure.

of a second doublet (modeled as two Gaussian components), with an average CS of 0.38 mm/s and an average QSD of 0.81 mm/s, corresponding $^{[6]}Fe^{3+}$. There is no evidence for $^{[4]}Fe^{3+}$. The resultant Fe^{3+}/Fe_{tot} ratio obtained from analysis of the spectral areas is 0.215(7), corresponding to 0.33 *apfu* Fe^{3+}, a high value compared to those obtained for other samples of astrophyllite-group minerals from a variety of intrusive complexes (average $Fe^{3+}/Fe_{tot} \approx 0.07$, P. Piilonen, unpubl. data).

X-RAY CRYSTALLOGRAPHY

A chemically homogeneous grain of type-I niobokupletskite ($0.21 \times 0.19 \times 0.02$ mm) was selected from those within the electron-microprobe epoxy mount for a single-crystal X-ray-diffraction study. X-ray powder-diffraction data were collected with a 114.6 mm Debye–Scherrer camera with Cu$K\alpha$ radiation (Ni-filtered), operating at 45 kV and 20 mA, and are presented in Table 4. X-ray intensity data were collected using the Siemens SMART (Siemens Molecule Analysis Research Tool) system at the University of Ottawa; it consists of a PLATFORM three-circle goniometer and a 1 K (diameter: 9 cm (512 pixel) charge-coupled device (CCD) area-detector. Data were collected at room temperature using monochromatic Mo$K\alpha$ X-radiation

TABLE 3. MÖSSBAUER SITE DISTRIBUTION PARAMETERS FOR TYPE-II NIOBOKUPLETSKITE

	δ_0 (mm/s)	δ_1	A (counts·mm/s)	A_-/A_+
Fe^{2+}	1.07(3)	0.03(1)	118600(1600)	1*
Fe^{3+}	0.38(3)	0*	32500(1300)	1*

		p (%)	$\langle\Delta\rangle$ (mm/s)	$\sigma\Delta$ (mm/s)
Fe^{2+}	comp. 1	46	2.24(5)	0.5(1)
	comp. 2	7(15)	1.98(2)	0.2(2)
	comp. 3	46(2)	2.47(4)	0.20(4)
Fe^{3+}	comp. 1	27	0.6(1)	0.2(2)
	comp. 2	73(3)	0.8(3)	0.7(1)

	<CS> (mm/s)	$<|\Delta|>$ (mm/s)	stdev $(|\Delta|)$	skew $(|\Delta|)$
Fe^{2+}	1.13	2.33	0.39	-0.41
Fe^{3+}	0.38	0.81	0.52	0.89

reduced $\chi^2 = 0.96$

Site populations (%): Fe^{2+} **78.5(7)** Fe^{3+} **21.5(7)**

* fixed value

TABLE 4. X-RAY POWDER-DIFFRACTION DATA
FOR NIOBOKUPLETSKITE

d_{meas}	d_{calc}	I_{obs}	I_{calc}	hkl	d_{meas}	d_{calc}	I_{obs}	I_{calc}	hkl
10.707	10.619	100	100	001	2.409	2.412	10	6	$\bar{1}41$
	10.532		38	010		2.403		6	$\bar{1}34$
9.883	9.826	<5	17	$0\bar{1}1$	2.322	2.325	10	4	$\bar{2}12$
	5.829		<1	$0\bar{1}2$	2.308	2.308	10	5	131
5.840	5.785	5	12	$02\bar{1}$		2.299		5	144
4.405	4.432	20	20	$\bar{1}11$	2.254	2.255	<5	<1	$05\bar{1}$
	4.367		5	$1\bar{2}0$		2.250		7	$\bar{2}13$
	4.346		3	101	2.222	2.223	<5	3	$\bar{2}41$
	4.335		7	$12\bar{1}$		2.216		2	$\bar{2}22$
4.100	4.098	<5	<1	012		2.203		2	$\bar{2}21$
	4.083		6	021	2.130	2.124	5	3	$\bar{1}42$
3.816	3.795	5	3	$\bar{1}21$		2.124		3	005
	3.778		2	$1\bar{1}2$	2.118	2.118	5	1	140
	3.761		6	$02\bar{3}$		2.115		3	$\bar{1}35$
3.536	3.540	50	40	003	2.056	2.060	<5	3	$2\bar{1}3$
	3.539		10	111	2.023	2.025	<5	3	132
3.294	3.281	20	13	$\bar{1}13$		2.017		3	$\bar{1}45$
	3.275		2	$03\bar{3}$	1.995	1.999	<5	2	$\bar{1}51$
3.147	3.137	<5	5	022		1.987		2	$\bar{2}14$
3.108	3.099	<5	11	$\bar{1}22$		1.983		2	$\bar{2}32$
	3.046		<1	$\bar{1}23$	1.933	1.930	<5	1	015
3.047	3.044	<5	10	$12\bar{3}$		1.928		2	$06\bar{3}$
	2.996		5	013		1.774		7	133
	2.993		2	$\bar{1}31$	1.769	1.767	5	7	$\bar{1}46$
2.988	2.980	<5	<1	031		1.764		2	$\bar{2}62$
2.887	2.886	5	5	$13\bar{3}$		1.762		1	330
	2.877		4	$0\bar{1}4$	1.751	1.750	<5	7	$\bar{2}15$
	2.876		6	112	1.660	1.659	5	11	$07\bar{3}$
	2.831		4	121	1.633	1.634	<5	4	$\bar{1}44$
2.824	2.822	<5	1	$1\bar{4}1$		1.634		2	$\bar{1}27$
	2.819		2	$\bar{1}32$		1.631		2	240
2.793	2.787	40	22	$\bar{1}31$		1.628		4	$\bar{1}37$
	2.784		23	$\bar{1}42$		1.628		2	$\bar{2}45$
2.677	2.679	30	19	$\bar{2}11$	1.589	1.589	5	9	$\bar{3}51$
	2.668		3	$\bar{1}14$		1.589		9	$\bar{3}22$
	2.655		10	004	1.575	1.575	<5	<1	$\bar{2}53$
2.587	2.587	40	19	130		1.575		<1	$\bar{2}72$
	2.580		18	$1\bar{4}3$		1.573		2	$3\bar{5}0$
2.503	2.504	20	16	212		1.572		1	$3\bar{2}3$

$CuK\alpha$ radiation, Ni-filtered, 45 kV, 20 mA, 24-hour exposure, Debye–Scherrer camera 114.6 mm in radius, with intensities visually estimated. The values of d are expressed in Å.

TABLE 5. MISCELLANEOUS DATA: NIOBOKUPLETSKITE

Space Group $P\bar{1}$		Diffractometer	SIEMENS CCD
a (Å)	5.4303(9)	Radiation	$MoK\alpha$ (40 kV, 30 mA)
b	11.924(2)	Crystal Shape	plate
c	11.747(2)	Crystal Size	0.21 x 0.19 x 0.02 mm
α (°)	112.927(3)	μ (MoKα)	5.33 cm^{-1}
β	94.750(3)	Min/Max Trans.	0.343/0.664
γ	103.175(3)	$|E^2-1|$	0.985
V (Å^3)	669.5(3)	CFOM	1.08
Z	1		

Chemical Formula $K_2Na(Mn,Zn,Fe)_7(Nb,Zr,Ti)_2Si_8O_{26}(OH)_4(O,F)$
2θ Range $\quad$ $4.82 \leq 2\theta \leq 57.26$
Min/Max Indices $\quad$ $-7 \leq h \leq 7, -11 \leq k \leq 16, -15 \leq l \leq 15$
No. of Unique Reflections $\quad$ 3023
No. of Observed Reflections $\quad$ 1779
Criterion for Observed Reflections $\quad$ $F_o > 4\sigma(F_o)$
Final R (%) $\quad$ 5.97
wR^2 (%) $\quad$ 19.12
$R = \Sigma(|F_o|-|F_c|)/\Sigma|F_o|$
$wR^2 = [\Sigma(w)F_o^2 - F_c^2)^2/\Sigma[w(F_o^2)^2]^{1/2}, w = 1/\sigma^2(F_o)$

(40 kV, 30 mA) and a fixed detector-crystal distance of 12.621 cm. A frame width (ω) of 0.3° and count exposure times of 30 seconds per frame were the standard setting. A hemisphere of data was collected for $4.82 \leq 2\theta \leq 57.26$, with minimum and maximum indices $-7 \leq h \leq 7$, $-11 \leq k \leq 16$, and $-15 \leq l \leq 15$. The data were reduced, filtered, integrated, and corrected for Lorentz, polarization and background effects using the Siemens program SAINT. A Ψ-scan data set of 724 reflections was used during absorption corrections, using the program XPREP with the crystal modeled as an ellipsoid using the program XPREP. The merging R decreased from 14.14% before the absorption correction to 7.89% after the absorption correction, giving minimum and maximum transmission-factors of 0.343 and 0.664, respectively. Phasing of a set of normalized structure-factors gave a mean value $|E^2 - 1|$ of 0.985, suggesting the centrosymmetric space-group $P\bar{1}$, a feature consistent with other studies of triclinic astrophyllite-group minerals (Peng & Ma 1963, Woodrow 1967, Christiansen *et al.* 1998). Information pertinent to the

data collection and crystal structure can be found in Table 5. The structure of niobokupletskite was refined by least-squares methods using the SHELXL–93 set of programs (Sheldrick 1993), with starting parameters taken from Christiansen *et al.* (1998) for kupletskite from Kangerdlugssuaq, Greenland. During the initial refinement, Mn, the dominant octahedrally coordinated cation indicated by the analytical results, was assigned to $M(1) – M(4)$, whereas Nb was assigned to the D site on the basis of the analytical data. Refinement of the site-occupancy factors resulted in values less than unity for $M(1)$ and D, and values greater than unity for $M(2)$, $M(3)$, and $M(4)$. Sodium was assigned to $M(1)$, and Ti was assigned to D. Zinc, a heavier X-ray scatterer than Mn and the second most abundant element in C according to the electron-microprobe data, was assigned to $M(2)$, $M(3)$ and $M(4)$; the pattern of order of Zn over these four sites is discussed below. The shape of the anisotropic displacement ellipsoid of the site to which K is assigned suggests that it is positionally disordered; it was therefore modeled as two split sites, [9]$K(1a)$ and [10]$K(1b)$, displaced 0.36 Å from each other along X. Displacement factors for $K(1a)$ and $K(1b)$ were constrained to be equal and refined isotropically. The structure refined to $R = 9.40\%$ and $wR^2 = 26.11\%$ with isotropic displacement factors, and to $R = 5.97\%$ and $wR^2 = 19.22\%$ with anisotropic displacement factors. An isotropic extinction correction was applied but did not improve the results. The high final R value is attributable to slippage along the {001} cleavage, imposed during extraction of the crystal from the epoxy mount, and also to microfractures observed in the crystal in BSE images (Fig. 1A). The final positional and isotropic displacement parameters are given in Table 6, and selected bond-lengths are given in Table 7. Bond-valence sums were calculated using parameters taken from Brese & O'Keeffe (1991) and can be found in Table 8. The observed and calculated structure-factors are available

TABLE 6. POSITIONAL AND DISPLACEMENT PARAMETERS AND SITE OCCUPANCIES FOR NIOBOKUPLETSKITE

Atom	x	y	z	sof	*U_{11}	U_{22}	U_{33}	U_{23}	U_{13}	U_{12}	U_{eq}
Mn(1)	0.8511(3)	0.2057(2)	0.4794(2)	0.91(1)	26(9)	138(11)	163(11)	67(8)	27(7)	31(7)	106(6)
Na	0.8511(3)	0.2057(2)	0.4794(2)	0.09(1)	26(9)	138(11)	163(11)	67(8)	27(7)	31(7)	106(6)
Mn(2)	0.2790(3)	0.0680(2)	0.4871(1)	0.90(3)	38(8)	164(11)	174(10)	91(8)	44(6)	39(7)	115(6)
Zn(2)	0.2790(3)	0.0680(2)	0.4871(1)	0.10(3)	38(8)	164(11)	174(10)	91(8)	44(6)	39(7)	115(6)
Mn(3)	0.4211(3)	0.3512(2)	0.4844(1)	0.85(3)	43(8)	154(11)	185(10)	88(8)	43(6)	35(7)	119(6)
Zn(3)	0.4211(3)	0.3512(2)	0.4844(1)	0.15(3)	43(8)	154(11)	185(10)	88(8)	43(6)	35(7)	119(6)
Mn(4)	0	0.5	0.5	0.33(2)	13(10)	131(14)	166(13)	55(10)	20(8)	-4(9)	110(8)
Zn(4)	0	0.5	0.5	0.17(2)	13(10)	131(14)	166(13)	55(10)	20(8)	-4(9)	110(8)
Nb	0.0749(2)	0.0818(1)	0.1865(1)	0.90(1)	4(5)	133(6)	178(6)	77(5)	37(4)	26(4)	100(4)
Ti	0.0749(2)	0.0818(1)	0.1865(1)	0.10(1)	4(5)	133(6)	178(6)	77(5)	37(4)	26(4)	100(4)
Si(1)	0.6786(6)	0.2745(3)	0.2314(3)	1.00	68(14)	186(18)	154(16)	103(14)	45(11)	60(12)	120(7)
Si(2)	0.8133(6)	0.5470(3)	0.2526(3)	1.00	95(14)	136(17)	146(16)	76(14)	23(12)	24(13)	122(7)
Si(3)	0.3765(6)	0.6737(3)	0.2552(3)	1.00	89(15)	167(18)	149(16)	84(14)	9(11)	18(13)	133(7)
Si(4)	0.5070(5)	0.9296(3)	0.2362(3)	1.00	49(14)	108(16)	139(15)	47(14)	21(11)	18(12)	103(7)
K(1a)	0.097(6)	0.278(1)	0.995(1)	0.41(6)							433(17)
K(1b)	0.164(4)	0.2754(8)	0.9956(8)	0.48(6)							433(17)
Rb(1b)	0.164(4)	0.2754(8)	0.9956(8)	0.065							433(17)
Na	0.5	0	0	0.45	148(39)	200(46)	147(39)	46(33)	-11(28)	33(29)	179(24)
O(1)	0.728(1)	0.3194(7)	0.3832(7)	1.00	28(33)	226(45)	165(39)	102(37)	33(29)	73(32)	126(16)
O(2)	0.146(1)	0.1600(8)	0.3682(7)	1.00	134(40)	167(45)	176(41)	74(37)	21(32)	45(35)	158(17)
O(3)	0.130(1)	0.3931(7)	0.5949(6)	1.00							88(15)
OH(4)	0.295(1)	0.4631(8)	0.3991(7)	1.00	102(36)	210(44)	146(38)	84(36)	74(30)	114(34)	134(16)
OH(5)	0.993(1)	0.1179(7)	0.5944(7)	1.00	104(37)	133(42)	142(38)	23(35)	67(30)	13(32)	139(16)
O(6)	0.559(1)	0.2576(7)	0.5915(6)	1.00	24(32)	161(42)	107(36)	60(34)	24(28)	19(30)	96(16)
O(7)	0.573(1)	0.0134(7)	0.3865(7)	1.00	37(33)	74(39)	184(40)	61(34)	0(29)	-11(29)	102(16)
O(8)	0.072(1)	0.5915(8)	0.2004(7)	1.00	184(43)	284(52)	222(47)	91(43)	131(37)	36(39)	235(20)
O(9)	0.250(2)	0.043(1)	0.8260(9)	1.00	268(53)	597(76)	210(49)	30(51)	51(42)	-337(52)	486(33)
O(10)	0.433(2)	0.4144(8)	0.7988(7)	1.00	215(46)	359(57)	186(46)	98(44)	22(37)	116(42)	254(21)
O(11)	0.129(2)	0.803(1)	0.8297(9)	1.00	683(78)	595(75)	238(52)	182(55)	22(51)	534(67)	431(29)
O(12)	0.267(2)	0.954(1)	0.1723(9)	1.00	709(79)	516(72)	185(49)	-78(45)	-189(50)	526(65)	498(35)
O(13)	0.266(2)	0.6062(8)	0.8075(8)	1.00	508(63)	106(45)	140(41)	18(37)	35(39)	77(45)	266(22)
O(14)	0.571(2)	0.2206(8)	0.8024(8)	1.00	568(66)	88(45)	206(46)	58(40)	29(44)	-14(45)	311(24)
O(15)	0.385(2)	0.197(1)	0.1693(8)	1.00	308(55)	559(74)	240(50)	202(53)	-56(43)	-247(52)	431(30)
O(16)	0	0	0	0.50	76(52)	277(72)	213(62)	121(54)	65(42)	96(47)	172(35)

*$U_{ij} \times 10^4$

from the Depository of Unpublished Data, CISTI, National Research Council of Canada, Ottawa, Ontario K1A 0S2, Canada.

DESCRIPTION OF THE STRUCTURE

Astrophyllite-group minerals are generally triclinic (but also monoclinic) alkali titano-, zircono-, and niobosilicates that occur in SiO_2-oversaturated- and undersaturated alkaline rocks ranging in composition from alkali granites to peralkaline nepheline syenites. The crystal structure of astrophyllite was first determined by Peng & Ma (1963) and later elaborated on by Woodrow (1967). Since then, structural studies of members of the astrophyllite group have been performed by Christiansen et al. (1998; kupletskite) and Shi et al. (1998;

TABLE 7. SELECTED INTERATOMIC
DISTANCES (Å) FOR NIOBOKUPLETSKITE

$M(1)$-O(2)	2.179(8)	$T(1)$-O(11)	1.585(9)
$M(1)$-O(6)	2.190(7)	$T(1)$-O(15)	1.595(9)
$M(1)$-OH(5)	2.194(8)	$T(1)$-O(1)	1.628(8)
$M(1)$-O(3)	2.209(7)	$T(1)$-O(13)	1.631(9)
$M(1)$-O(7)	2.221(7)	$<T(1)$-O>	1.604
$M(1)$-O(1)	2.247(7)		
$<M(1)$-O>	2.207	$T(2)$-O(13)	1.614(9)
		$T(2)$-O(3)	1.620(7)
$M(2)$-OH(5)	2.124(7)	$T(2)$-O(8)	1.638(8)
$M(2)$-O(7)	2.133(8)	$T(2)$-O(10)	1.654(8)
$M(2)$-OH(5)	2.152(8)	$<T(2)$-O>	1.629
$M(2)$-O(6)	2.211(7)		
$M(2)$-O(2)	2.252(8)	$T(3)$-O(6)	1.629(7)
$M(2)$-O(7)	2.254(7)	$T(3)$-O(14)	1.630(9)
$<$M2-O>	2.188	$T(3)$-O(10)	1.630(9)
		$T(3)$-O(8)	1.645(8)
$M(3)$-O(1)	2.143(7)	$<T(3)$-O>	1.634
$M(3)$-OH(4)	2.145(7)		
$M(3)$-O(3)	2.151(7)	$T(4)$-O(9)	1.591(9)
$M(3)$-O(6)	2.169(7)	$T(4)$-O(12)	1.591(9)
$M(3)$-OH(4)	2.210(8)	$T(4)$-O(14)	1.607(9)
$M(3)$-O(2)	2.232(8)	$T(4)$-O(7)	1.613(8)
$<M(3)$-O>	2.175	$<T(4)$-O>	1.601
$M(4)$-OH(4)	2.097(7) x 2	K(1a)-O(12)	2.83(2)
$M(4)$-O(1)	2.149(8) x 2	K(1a)-O(11)	2.85(2)
$M(4)$-O(3)	2.181(7) x 2	K(1a)-O(15)	3.04(2)
$<M(4)$-O>	2.142	K(1a)-O(9)	3.07(2)
		K(1a)-O(14)	3.25(3)
D-O(2)	1.929(8)	K(1a)-O(16)	3.26(1)
D-O(16)	1.981(1)	K(1a)-O(13)	3.27(3)
D-O(9)	1.987(8)	K(1a)-O(8)	3.41(2)
D-O(15)	1.994(8)	$<K$(1a)-O>	3.12
D-O(12)	1.998(9)		
D-O(11)	2.001(9)	K(1b)-O(15)	2.84(2)
$<D$-O>	1.982	K(1b)-O(9)	2.88(2)
		K(1b)-O(12)	2.99(2)
Na-O(12)	2.64(1) x 2	K(1b)-O(11)	3.00(2)
Na-O(9)	2.64(1) x 2	K(1b)-O(16)	3.224(9)
Na-O(11)	2.66(1) x 2	K(1b)-O(14)	3.29(2)
Na-O(15)	2.66(1) x 2	K(1b)-O(13)	3.35(2)
Na-O(16)	2.715(0) x 2	K(1b)-O(10)	3.56(1)
$<$Na-O>	2.66	K(1b)-O(8)	3.57(2)
		$<K$(1b)-O>	3.19

monoclinic magnesium astrophyllite). All triclinic species have the general formula $A_2BC_7D_2T_8O_{26}(OH)_4$(F, O,OH), where A = [13]K, Rb, Cs, $\square$ or H_3O; B = [10]Na and Ca; C = four distinct octahedrally coordinated sites [$M(1)$, $M(2)$, $M(3)$ and $M(4)$], D = [6]Ti, Nb or Zr, and T = [4]Si and Al. Following a modular approach applied to structures of similar titanosilicates (*i.e.*, nafertisite, lamprophyllite), Ferraris *et al.* (1996) have described astrophyllite-group minerals as heterophyllosilicates having a *HOH*-structure (Fig. 4) consisting of a sheet of close-packed octahedra (*O*-sheet; Fig. 5), composed of MnO_6, FeO_6, NaO_6 or MgO_6 octahedra, sandwiched between two heterogeneous sheets (*H*-sheets). The *H*-sheet consists of open-branched *zweier* single chains of [Si_4O_{12}]$^{8-}$ (Liebau 1985) running parallel to *X*, which are in turn cross-linked by corner-sharing DO_6 octahedra (*D*: Nb,Ti,Zr) (Fig. 6). Individual DO_6 octahedra are linked across the interlayer *via* a common apical anion [O(16), special position 1*a* (0,0,0)]. A misfit exists be-

tween the *O*- and *H*-sheets, resulting in tilting and rotation of SiO_4 tetrahedra and distortion or corrugation of the *O*-sheet. The degree to which this misfit occurs is directly dependent on the composition of the *O*-sheet and decreases with increasing size of the *O*-sheet cations (Woodrow 1967, Christiansen *et al.* 1998, Shi *et al.* 1998).

The interlayer

The interlayer of niobokupletskite contains both Na and K in two distinct sites. Sodium is [10]-coordinated and located between bridging apices of the NbO_6 octahedra. Bond lengths range from 2.64(1) to 2.715(0) Å. Refinement of the site-occupancy factor gives 0.90, suggesting the presence of vacancies or of a lighter scatterer (*e.g.*, H_2O, H_3O^+). Electron-microprobe data indicate 1.23 *apfu* of Na in niobokupletskite, suggesting an "excess" of Na if compared with results obtained from the structure refinement. This excess Na has been accounted for in the $M(1)$ octahedral site. Substitution of Ca for Na within the interlayer is common in more Fe-rich astrophyllite-group minerals (*e.g.*, Christiansen *et al.* 1998), but was not detected in type-I niobokupletskite. Bond lengths to the two split sites to which K is assigned are as follows: [9]K(1a) 2.83(2) to 3.41(2) Å, [10]K(1b) 2.84(2) to 3.57(2) Å. A high site-occupancy factor for K(1b) (0.62) indicates the presence of a heavier scatterer. Rubidium, determined by electron-microprobe analysis to be 0.13 *apfu*, was therefore assigned to this site.

The O sheet

The *O* sheet of niobokupletskite is identical to that in kupletskite, except for additional Zn, Fe, Na and Mg. In the largest and least distorted of the four octahedra, $M(1)$, the *M* cation is coordinated by five O^{2-} and one OH^- [OH(5)], with a $<M(1)$–O> distance of 2.207 Å [volume: 13.990 Å^3, calculated in IVTON (Balić-Žunić & Vickovic 1996); distortion (Δ): 1.041, calculated using the equation for quadratic elongation (Brown & Shannon 1973)]. The $M(1)$ site in niobokupletskite is slightly larger than that of kupletskite ($<M(1)$–O>: 2.203 Å, volume: 13.858 Å^3; Christiansen *et al.* 1998) owing to the presence of Na. Site-scattering refinements (SREF) of $M(1)$ consistently yielded occupancies less than unity, indicating the presence of a weaker scatterer or of vacancies. Electron-microprobe data, and a low site-occupancy factor for the site assigned to Na, indicate an "excess" of Na. The occupancy of $M(1)$ was therefore refined with both Mn and Na, resulting in site populations consistent with the EMPA data (SREF: 0.18 *apfu*, EMPA: 0.28 *apfu*) and a bond-valence sum of 1.95 *vu*. The presence of Na within the $M(1)$ site is not an uncommon feature in astrophyllite-group minerals. For example, magnesium astrophyllite (Shi *et al.* 1998), which is monoclinic, exhibits a dominance of Na within

TABLE 8. EMPIRICAL BOND-VALENCES (vu) FOR NIOBOKUPLETSKITE[*]

	M(1)	M(2)	M(3)	M(4)	D	T(1)	T(2)	T(3)	T(4)	Na	K(1a)	K(1b)	Σ
O(1)	0.29		0.36	0.35^{X2}↓		0.99							1.99
O(2)	0.35	0.28	0.28		0.95								1.86
O(3)	0.32		0.36	0.32^{X2}↓			1.01						2.01
OH(4)			0.67	0.41^{X2}↓									1.08
OH(5)	0.34	0.76											1.10
O(6)	0.34	0.31	0.35					0.99					1.99
O(7)	0.31	0.66							1.03				2.00
O(8)							0.96	0.94			0.01	0.01	1.92
O(9)					0.79				1.09	0.10^{X2}↓	0.03	0.07	2.08
O(10)							0.92	0.98				0.02	1.92
O(11)					0.76	1.11				0.10^{X2}↓	0.06	0.06	2.09
O(12)					0.71				1.09	0.10^{X2}↓	0.06	0.05	2.01
O(13)						0.98	1.03				0.02	0.03	2.06
O(14)								0.98	1.05		0.02	0.04	2.09
O(15)					0.78	1.08				0.10^{X2}↓	0.03	0.08	2.07
O(16)					0.81^{X2}→					0.08^{X3}→	0.02^{X2}→	0.02^{X2}→	1.86
Σ	1.95	2.01	2.02	2.16	4.80	4.16	3.92	3.89	4.26	0.96	0.25	0.38	

[*] constants from Brese & O'Keefe (1991)

Note: Valences for M and D sites were calculated using the following weighted averages: M(1): (Mn$_{0.91}$Na$_{0.09}$),
M(2): (Mn$_{0.9}$Zn$_{0.1}$), M(3): (Mn$_{0.85}$Zn$_{0.15}$), M(4): (Mn$_{0.33}$Zn$_{0.17}$), D: (Nb$_{0.90}$Ti$_{0.10}$), K(1b): (K$_{0.48}$Rb$_{0.06}$)

a single octahedrally coordinated site equivalent of $M(1)$ in the triclinic species; this dominance has also been noted in other astrophyllite-group minerals from Mont Saint-Hilaire (P. Piilonen, unpubl. data). Substitution of Na for Mn in octahedral coordination, although not common, also has been noted in other minerals, including samuelsonite (Moore & Araki 1977), barytolamprophyllite (Rastsvetaeva & Dorfman 1995), vuonnemite (Ercit *et al.* 1998), and in alkali clinoamphiboles from Mont Saint-Hilaire (Taylor 1999). This phenomenon may be attributable to high activities of Na within the crystallizing magma.

The $M(2)$, $M(3)$ and $M(4)$ sites are larger and less distorted than those observed in kupletskite, probably owing to the increased extent of substitution of Mn for Fe in niobokupletskite. The $M(2)$ and $M(3)$ sites have a *cis* configuration [$M(2)$: OH(5) $\times$ 2, $M(3)$: OH(4) $\times$ 2], with average <M–O> distances of 2.188 and 2.175 Å respectively, whereas $M(4)$ is a *trans* site [OH(4) $\times$ 2], with an average <$M(4)$–O> distance of 2.142 Å. The $M(2)$ octahedra, the most distorted in the O-sheet of astrophyllite-group minerals (Δ: 6.059), are unusual, as they form continuous zigzag chains parallel to the X axis; all other M sites share at most one common edge with crystallographically equivalent octahedra (Fig. 5). The combination of continuous chains of $M(2)$ octahedra and open-branched *zweier* single chains parallel to X in the H-sheet has a pronounced effect on the mor-

phology of astrophyllite-group minerals: a preferential elongation of crystals in the X direction, the development of a secondary, moderate parting along {010}, and the formation of acicular to tabular crystals.

Site-scattering refinements indicate departures from ideal Mn occupancies and the presence of a stronger X-ray scatterer in all of $M(2)$, $M(3)$ and $M(4)$. Zinc, the second most abundant octahedrally coordinated cation recorded in the EMPA data, was refined in all three of these sites, with the total site-occupancy constrained to be unity. Zinc populations are as follows: $M(2)$ 0.10, $M(3)$ 0.15, $M(4)$ 0.34, resulting in a total Zn content in agreement with that obtained by electron microprobe (SREF: 0.84, EMPA: 0.73 *apfu*). Bond-valence sums indicate these site-occupancy factors to be reasonable [$M(2)$: 2.01 *vu*, $M(3)$: 2.02 *vu*, $M(4)$: 2.16 *vu*]. Results of this refinement suggest that Zn, a cation significantly smaller than Mn ($^{[6]}$Zn^{2+}: 0.74 Å, $^{[6]}$Mn^{2+}: 0.83 Å; Shannon 1976) preferentially orders at $M(4)$, the smallest of the four M sites [volumes: $M(2)$ 13.687, $M(3)$ 13.460, $M(4)$ 12.902 Å^3].

The H-sheet

There are four distinct tetrahedrally coordinated sites (T) in the niobokupletskite structure. As EMPA results reveal only minor Al^{3+} (average: 0.34 *apfu*), and Mössbauer spectroscopy did not indicate $^{[4]}$Fe^{3+}, all four
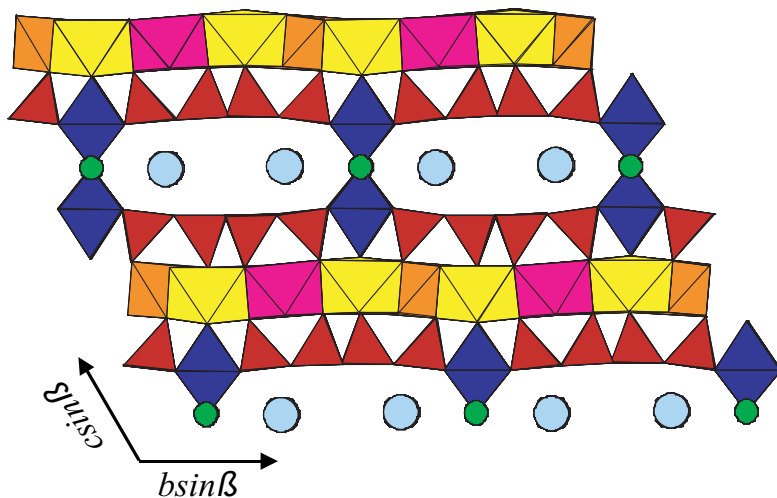
FIG. 4. The structure of niobokupletskite showing the *HOH* structure and interlayer cations (K light blue, Na green). The coloring of the polyhedra are as follows: *T* red, *D* dark blue, *M*(1) yellow, *M*(2) orange, *M*(4) deep pink. Note that *M*(3) is not observed in this projection.

T sites were modeled with only Si^{4+} during the structure refinement. Bond lengths within the four tetrahedral sites range from 1.585(9) to 1.654(8) Å. In niobokupletskite, *T*(1) and *T*(4) each share two basal, non-bridging (nb) oxygen atoms with the basal plane of the NbO_6 octahedra [*T*(1): O(15), O(11) and *T*(4): O(9), O(12)]. Shorter bond-lengths to these basal oxygen atoms (<*T*(1)–O_{nb}> 1.590 Å, <*T*(4)–O_{nb}> 1.591 Å) result in a tilting of *T*(1) and *T*(4) 7.73° and 7.65° out of the

(001) plane, respectively, toward the NbO_6 octahedra. However, the *T*(2) and *T*(3) bridging tetrahedra, which do not share common oxygen atoms with the NbO_6 octahedra, are tilted only 7.11 and 7.05° out of the (001) plane, respectively, and display slightly longer basal <*T*–O> bond lengths than *T*(1) and *T*(4) (<*T*(2)–O_{basal}> 1.629 Å, <*T*(3)–O_{basal}> 1.635 Å).

In niobokupletskite, bond valence sums (Table 8) indicate the presence of a divalent anion in the O(16)
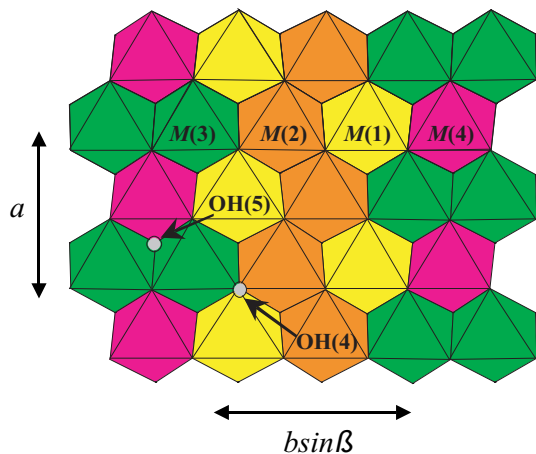
FIG. 5. The *O*-sheet of niobokupletskite showing the individual *M* octahedra. Note the continuous zigzag chains of *M*(2) octahedra (orange) parallel to the *X* axis (*a*).
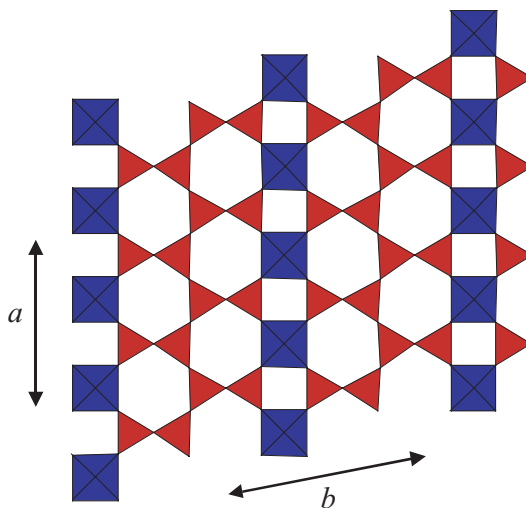
FIG. 6. The *H*-sheet of niobokupletskite showing open-branched *zweier* single chains of $[Si_4O_{12}]^{8-}$ parallel to the *X* axis (*a*) (red) cross-linked by NbO_6 octahedra (blue).

position (1.86 *vu*), unlike Ti-dominant astrophyllite-group minerals, for which bond-valence calculations indicate a monovalent anion (OH or F: Christiansen *et al.* 1998). The incorporation of O^{2-} at the O(16) position is required in order to balance the excess positive charge attributable to Nb^{5+} resulting from the $Nb^{5+} \Leftrightarrow Ti^{4+}$ substitution. The following coupled substitution is therefore suggested for the incorporation of Nb^{5+} into the structure:

$$Ti^{4+} + F^- \text{ or } OH^- \Leftrightarrow Nb^{5+} + O^{2-} \qquad (1)$$
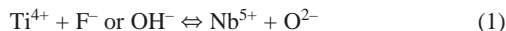
The same mechanism of substitution has been suggested for the incorporation of Ti and F into the wöhlerite structure (Mellini & Merlino 1979). The presence of O^{2-} at the O(16) position results in a local increase in symmetry along Z within the DO_6 octahedra due to the presence of a strong O(2)–Nb–O(16) bond rather than the weaker, asymmetrical O(2)–Ti–F bond observed in Ti-dominant astrophyllite-group minerals. The subsequent shortening of D–O(16) and lengthening of D–O(2) are direct results of Nb being positionally more central within the polyhedra, rather than being displaced along Z toward the O-layer, as is the case with Ti-dominant polyhedra (P. Piilonen, unpubl. data). The <O(16)–D–O$_{basal}$> bond angles are increased [85.4°, niobokupletskite; 80.8°, kupletskite (Christiansen *et al.* 1998)] and <O(2)–D–O$_{basal}$> are decreased [niobokupletskite: 94.6°; kupletskite: 99.2° (Christiansen *et al.* 1998)] as a result of this displacement. The net result of all these modifications is the significant decrease in distortion of the D polyhedra [Δ(niobokupletskite): 1.526 *versus* Δ(kupletskite): 17.840].

DISCUSSION

The proposed coupled substitution between kupletskite and niobokupletskite appears to be extensive. In samples of Mn-dominant astrophyllite-group minerals

from a variety of SiO_2-undersaturated complexes, including Mont Saint-Hilaire, Lovozero (Kola Peninsula, Russia) and the Oslo rift (Langesundsfjord area, Norway), a strong negative correlation exists between levels of Nb and Ti (Fig. 7) and between Nb and F (Fig. 8). The average Nb content of Mn-dominant astrophyllite-group minerals from these localities ranges from 0.06 to 1.33 *apfu* (67% Nb-for-Ti substitution) with an average F content of 0.11 to 0.95 *apfu* (89% O-for-F substitution; P. Piilonen, unpubl. data).

The incorporation of Zn into the niobokupletskite structure, and into astrophyllite-group minerals in general, may offer an indication of the sulfur fugacity, $f(S_2)$, at the time of crystallization. Electron-microprobe analyses indicate a bimodal distribution of Zn in niobokupletskite (Table 1); type-I niobokupletskite contains 0.73 *apfu* Zn, whereas type-II and type-III niobokupletskite do not contain essential Zn (Table 2). Type-III niobokupletskite is associated with wurtzite and genthelvite [$Zn_4Be_3(SiO_4)_3S$], two of only six Zn-bearing species to be described from Mont Saint-Hilaire (Horváth & Gault 1990). The presence of a (Zn,S)-bearing species in association with Zn-free niobokupletskite (type III) and of Zn-bearing niobokupletskite in the absence of associated Zn–S species (type I), suggests that Zn readily enters into the astrophyllite-group mineral structure in conditions where the $f(S_2)$ is too low to allow for the crystallization of a separate Zn–S species. The presence of wurtzite (the S-deficient hexagonal polymorph of ZnS) rather than sphalerite is of interest in this respect. Hydrothermal synthesis studies of the univariant wurtzite–sphalerite boundary have shown wurtzite to be stable at low $f(S_2)$ ($< 10^{-10}$ atm), and over a wide range of temperatures, as low as 100°C in diagenetic environments, thus contradicting the previously established inversion temperature of 1020°C (Scott & Barnes 1972). At higher values of $f(S_2)$ ($> 10^{-10}$ atm) and low temperatures (<465°C), sphalerite is the dominant ZnS polymorph. Sphalerite is ubiquitous at Mont
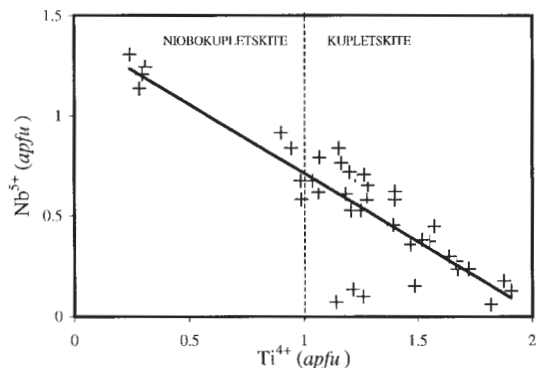

FIG. 7. Content of Ti^{4+} *versus* that of Nb^{5+} in the kupletskite–niobokupletskite solid-solution series. (Linear fit, R^2: 0.742).
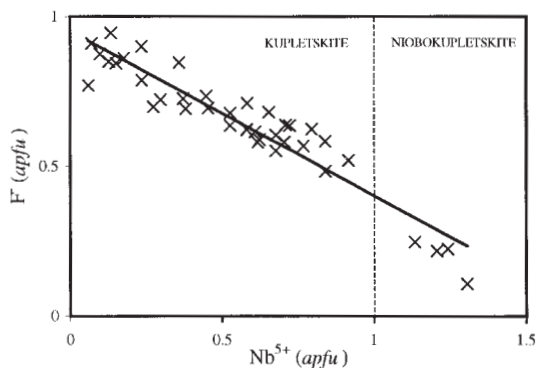

FIG. 8. Content of Nb^{5+} *versus* that of F^- in the kupletskite–niobokupletskite solid-solution series. (Linear fit, R^2: 0.893).

Saint-Hilaire as a late-stage phase in all the microenvironments, most commonly associated with other S-bearing species (*i.e.*, pyrite, pyrrhotite; Horváth & Gault 1990). The absence of sphalerite in samples containing niobokupletskite suggests that the $f(S_2)$ was too low to permit the formation of sphalerite, resulting in the formation of either S-deficient wurtzite or of zincian niobokupletskite.

The controls on the distribution of high-field-strength elements in the magma, and subsequently into alkali titano-, zircono- and niobosilicates such as those of the astrophyllite group, may contribute to an understanding of the parageneses of these minerals. For example, in peralkaline systems, zirconium shows a high solubility and a highly incompatible nature in the melt until the final stages of crystallization (Bowden 1966, Larsen 1973, Watson 1979, Dunn & McCallum 1982, Linthout 1984, Rubin *et al.* 1993). The high solubility of Zr in alkali-rich magmas can be attributed to the fact that Zr acts as a network modifier (Linthout 1984). An increase in the alkali content in the melt (Na + K) results in an increase in the proportion of non-bridging oxygen atoms to which Zr will preferentially bond, inhibition of [7]Zr and [8]Zr, and promotion of [6]Zr, leading to the incorporation of minor Zr into silicates such as pyroxenes and amphiboles, which have [6]-coordinated sites similar to those occupied by Zr in the melt polymers (*e.g.*, aegirine; Piilonen *et al*. 1998). Decreasing temperature, increased Ca, and increased $f(O_2)$ result in melt polymerization, decreased solubility of Zr, increased bonding between ZrO_6 and SiO_4 groups, and the formation of charge-balanced [6]Zr–O–(Si,Na) bonds within the melt (Linthout 1984, Farges *et al*. 1994). In all samples of niobokupletskite, the Zr:Ti ratio is greater than one (Zr/Ti: 1.38 to 1.91), suggesting that conditions were such to allow for decreased Zr solubility and preferential incorporation of Zr rather than Ti into the niobokupletskite structure. The high Fe^{3+}/Fe_{tot} ratio obtained by Mössbauer spectroscopy and the coupled substitution of Nb^{5+} and O^{2-} in the niobokupletskite series both suggest a highly oxidizing environment of formation of niobokupletskite. As such, it appears that Zr and Nb may behave similarly in a peralkaline melt, unlike Zr and Ti which behave independently and either partition into discrete Zr or Ti phases or else are strongly ordered into separate sites in a given mineral structure (Pyatenko & Voronkov 1978). The late-stage development of (Ca+Si+Nb)-bearing pyrochlore-group minerals in fractures within both niobokupletskite and primary kupletskite, and the presence of abundant late-stage catapleiite in association with niobokupletskite, suggest an increase in the (Ca+Zr+Nb) concentration during the final stages of crystallization from a residual melt, followed by the formation of niobo- and zirconosilicates. Zirconium-rich niobokupletskite may represent an intermediate phase between early Zr-rich pyroxene and late-stage Zr–Nb minerals (*e.g*., catapleiite, franconite). The source of Nb in niobokupletskite may be attributed to the local dissolution of primary Nb-rich kupletskite (on which fibers of the former have nucleated) or Nb-bearing minerals such as those of eudialyte group. More information regarding the distribution of Nb at Mont Saint-Hilaire is required before these hypotheses can be tested.

REFERENCES

ADAMS, F.D. (1903): The Monteregian Hills – a Canadian petrological province. *J. Geol.* **11**, 239- 282.

BALIĆ-ŽUNIĆ, T. & VICKOVIĆ, K. (1996): IVTON. A program for the calculation of geometrical aspects of crystal structures and some crystal chemical applications. *J. Appl. Crystallogr.* **29**, 305-306.

BOWDEN, P. (1966): Zirconium in Younger Granites of northern Nigeria. *Geochim. Cosmochim. Acta* **30**, 985-993.

BRESE, N.E. & O'KEEFFE, M. (1991): Bond-valence parameters for solids. *Acta Crystallogr.* **B47**, 192-197.

BROWN, I.D. & SHANNON, R.D. (1973): Empirical bond strength – bond length curves for oxides. *Acta Crystallogr.* **A29**, 266-282.

CHRISTIANSEN, C.C., JOHNSEN, O. & STÅHL, K. (1998): Crystal structure of kupletskite from the Kangerdlugssuaq intrusion, East Greenland. *Neues Jahrb. Mineral., Monatsh.*, 253-264.

DUNN, T. & MCCALLUM, I.S. (1982): The partitioning of Zr and Nb between diopside and melts in the system diopside – albite – anorthite. *Geochim. Cosmochim. Acta* **46**, 623-629.

EFIMOV, A.F., DUSMATOV, V.D., GANZEEV, A.A. & KATAEVA, Z.T. (1971): Cesium-kupletskite, a new mineral. *Dokl. Acad. Sci. USSR, Earth Sci. Sect.* **197**, 140-143.

ERCIT, T.S., COOPER, M.A. & HAWTHORNE, F.C. (1998): The crystal structure of vuonnemite, $Na_{11}Ti^{4+}Nb_2(Si_2O_7)_2$ $(PO_4)_2O_3(F,OH)$, a phosphate-bearing sorosilicate of the lomonosovite group. *Can. Mineral.* **36**, 1311-1320.

FARGES, F., BROWN, G.E., Jr. & VELDE, D. (1994): Structural environment of Zr in two inosilicates from Cameroon: mineralogical and geochemical implications. *Am. Mineral.* **79**, 838-847.

FARMER, V.C. (1974): Infrared Spectra of Minerals. *Mineral. Soc., Monogr.* **4**.

FERRARIS, G., IVALDI, G., KHOMYAKOV, A.P., SOBOLEVA, S.V., BELLUSO, E. & PAVESE, A. (1996): Nafertisite, a layer titanosilicate member of a polysomatic series including mica. *Eur. J. Mineral.* **8**, 241-249.

HORVÁTH, L & GAULT, R.A. (1990): The mineralogy of Mont Saint-Hilaire, Québec. *Mineral. Rec.* **21**, 284-359.

HUBEI GEOLOGIC COLLEGE, X-RAY LABORATORY (1974): The crystal chemistry of astrophyllite-group minerals. *Sci. Geol. Sinica* **1**, 18-33 (in Chinese).

KAPUSTIN, YU.L. (1973): Zircophyllite, the zirconium analogue of astrophyllite. *Int. Geol. Rev.* **15**, 621-625.

LAGAREC, K. & RANCOURT, D.G. (1998): RECOIL. Mössbauer spectral analysis software. Department of Physics, University of Ottawa, Ottawa, Canada.

LARSEN, L. (1973): Measurement of solubility of zircon $(ZrSiO_4)$ in synthetic granitic melts. *Trans. Am. Geophys. Union (Eos)* **54**, 479 (abstr.).

LIEBAU, F. (1985): *Structural Chemistry of Silicates: Structure, Bonding and Classification*. Springer-Verlag, Berlin, Germany.

LINTHOUT, K. (1984): Alkali-zirconosilicates in peralkaline rocks. *Contrib. Mineral. Petrol.* **86**, 155-158.

MANDARINO, J.A. (1981): The Gladstone–Dale relationship. IV. The compatibility concept and its application. *Can. Mineral.* **19**, 441-450.

MELLINI, M. & MERLINO, S. (1979): Refinement of the crystal structure of wöhlerite. *Tschermaks Mineral. Petrogr. Mitt.* **26**, 109-123.

MOORE, P.B. & ARAKI, T. (1977): Samuelsonite: its crystal structure and relation to apatite and octacalcium phosphate. *Am. Mineral.* **62**, 229-245.

NICKEL, E.H., ROWLAND, J.F. & CHARETTE, D.J. (1964): Niobophyllite – the niobium analogue of astrophyllite; a new mineral from Seal Lake, Labrador. *Can. Mineral.* **8**, 40-52.

PENG, C.C. & MA, C.S. (1963): Crystal structure of astrophyllite and a new type of band silicate radical. *Sci. Sinica* **12**, 272-276.

PIILONEN, P.C., MCDONALD, A.M. & LALONDE, A.E. (1998): The crystal chemistry of aegirine from Mont Saint-Hilaire, Quebec. *Can. Mineral.* **36**, 779-791.

PYATENKO, Y.A. & VORONKOV, A.A. (1978): Comparative crystal-chemical functions of titanium and zirconium in mineral structures. *Int. Geol. Rev.* **20**, 1050-1058.

RANCOURT, D.G., MCDONALD, A.M., LALONDE, A.E. & PING, J.Y. (1993): Mössbauer absorber thickness for accurate site populations in Fe-bearing minerals. *Am. Mineral.* **78**, 1-7.

_____ & PING, J.Y. (1991): Voigt-based methods for arbitrary-shape static hyperfine parameter distributions in Mössbauer spectroscopy. *Nucl. Instrum. Methods Phys. Res.* **B58**, 85-97.

RASTSVETAEVA, R.K. & DORFMAN, M.D. (1995): Crystal structure of Ba-lamprophyllite in the isomorphous lamprophyllite–barytolamprophyllite series. *Kristallografiya* **40**, 1026-1029 (in Russ.).

RUBIN, J.N., HENRY, C.D., & PRICE, J.G. (1993): The mobility of zirconium and other "immobile" elements during hydrothermal alteration. *Chem. Geol.* **110**, 29-47.

SCOTT, S.D. & BARNES, H.L. (1972): Sphalerite–wurtzite equilibria and stoichiometry. *Geochim. Cosmochim. Acta* **36**, 1275-1295.

SEMENOV, E.I. (1956): Kupletskite – a new mineral of the astrophyllite group. *Dokl. Akad. Nauk SSSR* **108**, 933-936 (in Russ.).

SHANNON, R.D. (1976): Revised effective ionic radii and systematic studies of interatomic distances in halides and chalcogenides. *Acta Crystallogr.* **A32**, 751-767.

SHELDRICK, G.M. (1993): *SHELXL-93. Program for the Refinement of Crystal Structures*. University of Göttingen, Göttingen, Germany.

SHI, NICHENG, MA, ZHESHENG, LI, GUOWU, YAMNOVA, N.A. & PUSHCHAROVSKY, D.YU. (1998): Structure refinement of monoclinic astrophyllite. *Acta Crystallogr.* **B54**, 109-114.

TAYLOR, R. (1999): *The Crystal Chemistry of Amphiboles from Mont Saint-Hilaire, Québec*. B.Sc. thesis, Laurentian University, Sudbury, Ontario.

WATSON, B.E. (1979): Zircon saturation in felsic liquids: experimental results and applications to trace element geochemistry. *Contrib. Mineral. Petrol.* **70**, 407-419.

WIGHT, Q. & CHAO, G.Y. (1986): Mont Saint-Hilaire revisited. *Rocks and Minerals* **61**, 182-197.

WOODROW, P.J. (1967): The crystal structure of astrophyllite. *Acta Crystallogr.* **22**, 673-678.